Microstructure and electrochemical properties of the vanadium alloys after low-temperature nitrogen plasma treatment

Z.A. Duriagina [a,b], D.D. Ryzhak [a], V.V. Kulyk [a,*],
T.L. Tepla [a], I.A. Lemishka [a], L.I. Bohun [a]

[a] Lviv Polytechnic National University, 12 Bandera St., Lviv, 79013, Ukraine
[b] The John Paul II Catholic University of Lublin, 14 Racławickie Av., 20-950 Lublin, Poland
* Corresponding e-mail address: kulykvolodymyrvolodymyrovych@gmail.com
ORCID identifier: https://orcid.org/0000-0002-2585-3849 (Z.A.D.); https://orcid.org/0000-0001-5999-3551 (V.V.K.)

ABSTRACT

Purpose: The proposed research aims to determine the expediency of surface treatment of vanadium alloys of V-Cr and V-Ti systems due to irradiation of their surfaces with low-temperature nitrogen plasma using plasma torch NO-01.

Design/methodology/approach: The investigation of microstructure and X-ray fluorescence analysis (XRF) of the samples were performed using an electron microscope TESCAN Vega3. The microhardness (Vickers hardness) of the samples was measured before and after surface treatment. The study of corrosive properties of the surface layers was performed by an electrochemical impedance spectroscopy (EIS) method. Corrosion damages were identified using impedance dependences.

Findings: The microstructure of the surface layers of the V-8Ti, V-15Cr, and V-35Cr alloys in the initial state and after plasma treatment have been investigated. The chemical composition of the surface layers is determined and comparative measurements of the microhardness of these alloys are carried out. Corrosion-electrochemical properties (corrosion potentials, electrochemical impedance spectroscopy and constructed potential-dynamic polarization curves) of investigated alloys after treatment with nitrogen plasma are evaluated.

Research limitations/implications: The results obtained using laboratory samples should be checked at the conditions of power equipment operation.

Practical implications: This treatment has advantages over other methods of surface engineering since it provides strong surface plastic deformation and the possibility of formation of secondary phases resulting in increases in surface hardness and corrosion resistance.

Originality/value: Vanadium alloys have significant advantages over other structural materials due to their high thermal conductivity and swelling resistance, high strength and plasticity up to temperatures of 700-800°C, and good weldability.

Keywords: Vanadium alloys, Surface layers, Microhardness, Corrosion

RESEARCH PAPER

PROPERTIES

1. Introduction

It is known that the basic structural materials of power equipment are low-alloyed pearlite-grade steels, ferritic-martensitic and austenitic stainless steels, nickel alloys, titanium and vanadium alloys, and some non-ferrous copper-based alloys. Among these materials, preference is given to vanadium alloys by reliability criteria, economic factors and, in the case of nuclear and fusion energetics, an insignificant decay of the induced activity. Significant natural resources of vanadium, high melting point, high decay rate of the induced activity, resistance to oxidation at operating temperatures up to 600°C, low specific gravity and a number of other physical properties make it a promising structural material. Vanadium alloy have significant advantages over other structural materials due to their high thermal conductivity and swelling resistance, high strength and plasticity up to temperatures of 700-800°C, and good weldability. These properties are decisive when selecting vanadium alloys of V-Cr, V-Ti, and V-Cr-Ti systems for investigations [1].

The solution of the problem of protection of materials is especially important, since there are no materials with absolute resistance to corrosion-erosion impact of working environments. Known methods of surface protection include the following: coating, inhibition of the working environment, formation of the protective barrier layers on the surface of structural material that would inhibit the degradation of its properties. The controlled formation of the structural-phase state of the surface of materials for purposeful change of their properties will significantly increase the lifetime of machine parts and structural elements of power equipment, which in turn will ensure their reliability and safety [2, 3].

When the equipment is running in coolants (Pb and $Li_{17}Pb_{83}$ melts), protective layers, which include nitrides or oxynitrides (TiN, TiON, VN, VON, Fe_4N), exhibit better behaviour [4]. Research over the past two decades has shown that the V-4Cr-4Ti alloy is the main candidate material for nuclear and fusion energetics [5-10]. It should also be noted that vanadium alloys are now also regarded as attractive candidate materials for advanced sodium or gas cooled fast reactors because of its low neutron penalty relative to other materials having higher melting temperatures [11].

Vanadium alloys potentially have low induced activation characteristics, high-temperature strength, and high coefficients of thermal expansion. Optimization of the chemical composition of these alloys implies avoiding the use of niobium and molybdenum to maintain low activation.

It is known, that chromium increases the strength of vanadium at high temperature and titanium enhances plasticity of vanadium by absorbing interstitial impurities, mostly oxygen. However, excess chromium or titanium can lead to loss of plasticity [12,13]. The properties of vanadium alloys are sensitive to O, N, and C impurities, hydrogen and helium isotopes, and their excess causes degradation of overall mechanical properties. In typical V-4Cr-4Ti and V-5Cr-5Ti alloys the impurity content is as follows: O (0.015-0.09 wt.%), N (0.007-0.46 wt.%), and C (0.006-0.03 wt.%) [14,15].

2. Experimental procedures

Plasma treatment of the material surface was carried out on a plasmatron NO-01 (electromagnetic shock tube type) with a pulse of 1…5 µs duration at various plasma pressure. The energy of the pulse of the plasma radiation is inversely proportional to the plasma pressure, so the accelerating voltage of 34 kV allowed to change the energy of the pulse within 50…150 J/cm^2.

The investigation of microstructure and X-ray fluorescence analysis (XRF) of the samples were performed using an electron microscope TESCAN Vega3, because it is equipped with modern electronic optics based on unique 4-lens wideband optics with its own intermediate lens [16]. This function made it possible to perform qualitative research using the SE (secondary electrons) detector with 30 kV acceleration voltage, since in the backscattering mode (BSE) the images were not rendered. Chemical analysis of samples was performed with a minimal magnification using XRF, i.e. a method of analysis of fluorescence spectra of elements emitted by an adsorption of high-energy radiation. As a result of using SEM Vega3 3D Beam technology, we get unique stereoscopic images.

The microhardness (Vickers hardness) of the samples was measured using NOVOTEST TC-MKB 1. Besides, various devices such as polectors, forcipol 2v, Struers rotopol-1, and Struers LaboPress-1 for polishing and processing of samples were used.

The study of corrosive properties of the surface layers was performed by an electrochemical impedance spectroscopy (EIS) method. Corrosion damages were identified using impedance dependences.

Impedance measurements were performed at open circuit potential using a frequency response analyser Gill AC. The working area of the samples was 2.0 cm^2. The studies were performed in the frequency range of 10,000 Hz to 0.01 Hz with a superimposed amplitude of 10-30 mV. Figure 1 shows a schematic diagram of the installation for obtaining the impedance dependences from the surface of the alloys under study.

The potentiostat operation was controlled by software ACM Instruments Version 5 (Fig. 2). Impedance spectra [17] were constructed using a program ACM Analysis v4.
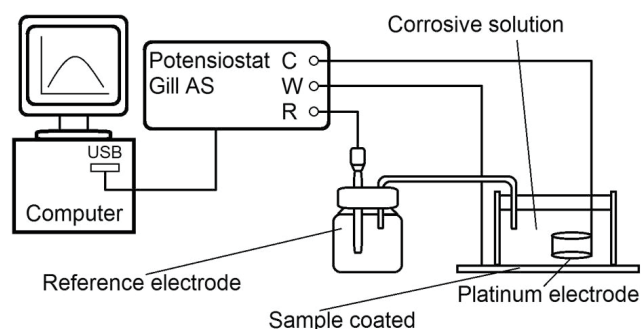

Fig. 1. Schematic diagram of the installation for obtaining the impedance dependences for vanadium alloys
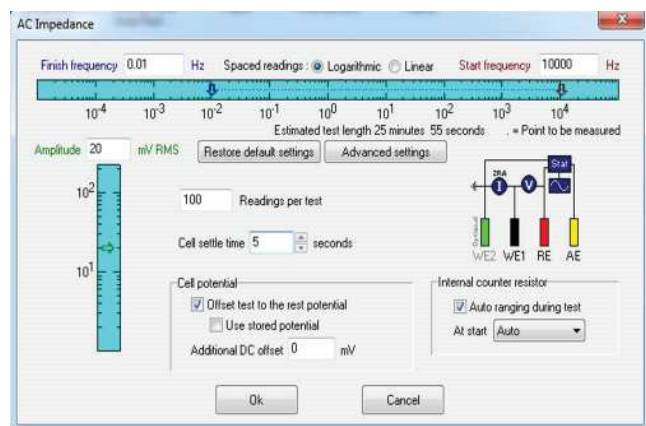

Fig. 2. Program interface (ACM Instruments Version 5) for the control of Gill AC potentiostat analyser with a measuring impedance spectra option

3. Results and discussion

The microstructure study of vanadium alloys after irradiation with low-temperature nitrogen plasma revealed periodically distributed areas of a darker colour on the surface of non-etched V-8Ti alloy samples. At a larger magnification, in these areas one can recognize dendritic crystals of various shapes and sizes (Fig. 3a). Hypothetical inclusions of nitrides or oxynitrides are recognized. It can be assumed that these areas were formed as a result of the uneven distribution of the energy of the hydrodynamic impact of nitrogen plasma, the density of which was found to be greater in these areas of the surface. This could also lead to the formation of the nitride phases (TiN, VN) by crystallization or condensation. The results of XRF analysis (Fig. 4a) carried out simultaneously with the metallographic research identify only the basic elements of the alloy: V (83.17 wt.%) and Ti (8.33 wt.%).

The presence of hypothetically formed nitride phases was not confirmed because of their small proportion. Besides, impurities such as Si (3.23 wt.%), O (3.33 wt.%), and Al (1.90 wt.%) were revealed in the V-8Ti alloy surface layer by the XRF analysis (Fig. 4a), and their amount would affect the mechanical properties of the alloy.

To confirm the presence of Si, we estimated its distribution over the material surface with corresponding software that uses a colour detection method (Fig. 3b). As a result, the presence of the Si admixture was confirmed, but the Al admixture was not detected.

The presence of oxygen suggests that, in addition to nitrides, oxides or oxynitrides (VO, V (ON), TiO$_2$, Ti(ON)) might be formed.

The microhardness of the V-8Ti alloy after nitrogen plasma treatment is 3400 MPa while the microhardness of the alloy without treatment is 1880 MPa (Tab. 1).

The alloy of the composition V-15Cr is characterized by a similar structure. At higher magnification, dendritic crystals are also seen (Fig. 3c), but they are larger in size than in the V-8Ti alloy (Fig. 3a). In contrast to the V-8Ti alloy, the results of XRF analysis (Fig. 4b) identify both the basic elements of the alloy, namely V (77.85 wt.%) and Cr (14.93 wt.%), and impurities: Si (1.95 wt.%), Al (1.76 wt.%), and O (3.51 wt.%). The presence of the Si impurity was not confirmed by the colour detection method because of its small proportion. Such low content of Si (1.95%) as compared to its content in the V-8Ti alloy (3.23%) can be the reason of not identifying by this method.

The microhardness of the V-15Cr alloy after nitrogen plasma treatment is 1950 MPa, and the microhardness of the alloy without treatment is 1630 MPa (Tab. 1).
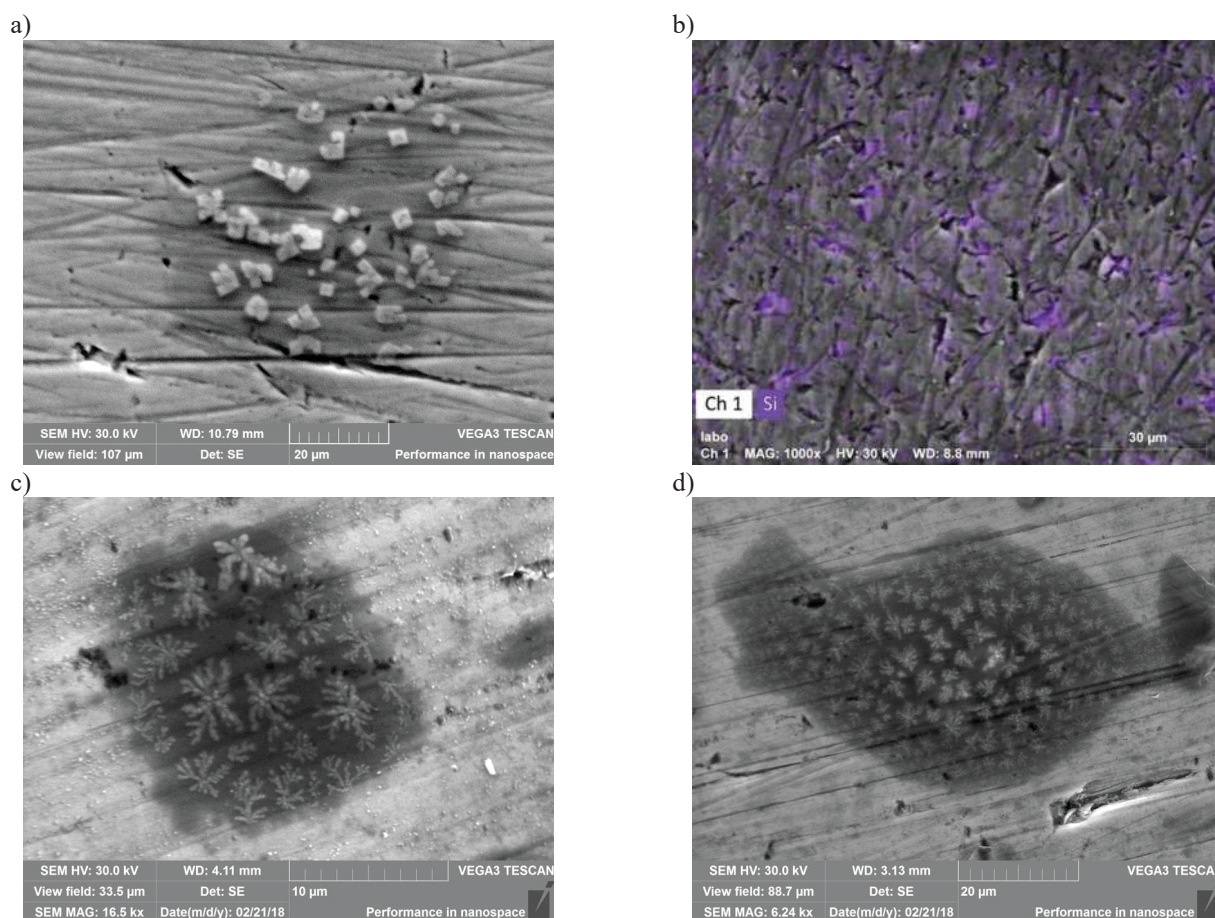
Fig. 3. The surface structure of the V-8Ti (a, b), V-15Cr (c) and V-35Cr (d) alloy after nitrogen plasma treatment (a, c, d – in the non-etched state; b – with the application of a colour detection method displaying areas of violet colour that correspond to Si impurities)

Table 1.
Microhardness of the vanadium alloys

Elemental composition	Microhardness HV, MPa	
	in the initial state	after plasma processing
V-8Ti	1880	3400
V-15Cr	1630	1950
V-35Cr	2120	2350

It was found that the surface microstructure of the V-35Cr alloy is slightly different from the previously investigated alloy, but the number of dark areas with dendritic crystals is larger (Fig. 3d). The results of the XRF (Fig. 4c) analysis of the V-35Cr alloy showed the presence of basic elements, namely V (62.38 wt.%) and Cr (34.63 wt.%), and impurities: Si (1.75 wt.%) and Al (1.24 wt.%). The presence of oxygen was not detected. It should be noted that the percentage of silicon and aluminium practically does not differ from the

determined for V-15Cr alloy. The microhardness of the V-35Cr alloy after nitrogen plasma treatment is 2350 MPa while the microhardness of the alloy without treatment is 2120 MPa (Tab. 1).

Corrosion tests of the alloys were performed in 3% NaCl aqueous solution, since in most cases their operation environment is the cooling aqueous medium containing Na^+ and Cl^- ions. Moreover, the concentration of NaCl in this solution is much higher than in the traditional water-cooled solution. As a result, these tests can appropriately assess the corrosion properties of the alloys.

The method of determination of electrode potentials allows to evaluate the ability of the alloy to repassivation after the violation of its passive state due to damage to the passive oxide film. If the potential of the metal in 3% NaCl aqueous solution is shifted to the positive side, this indicates the inhibition of the anode corrosion reaction. More negative values of the corrosion potential can be caused by lowering

of the rate of ionization reaction of the metal or the reduction of its corrosion resistance. For ordinary carbon steel, which is not passivated, the corrosion potential is in the range of -600 to -650 mV.
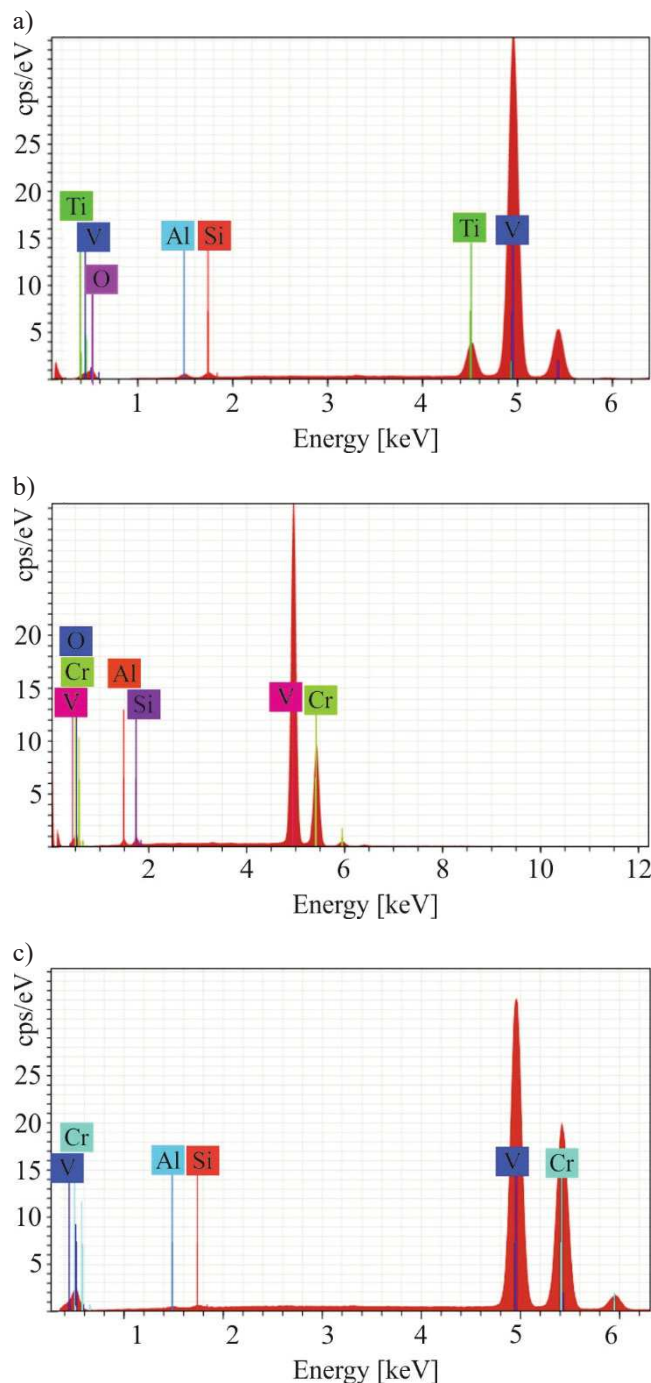
a)

b)

c)

Fig. 4. Results of the XRF analysis of the V-8Ti (a), V-15Cr (b) and V-35Cr (c) alloy surface

The kinetics of corrosion potentials of alloys V-8Ti, V-15Cr, and V-35Cr in 3% NaCl aqueous solution (Fig. 5) indicates their tendency to passivation. According to corrosion potential data, the V-8Ti alloy is the most corrosion-resistant. The value of its corrosion potential varies between -250 and -300 mV. The electrode potentials of both vanadium-chromium alloys are in the range of -330 to -370 mV. It should be noted that the increase in chromium content from 15 to 35 wt.% does not significantly affect the corrosion potential of the V-Cr alloy.
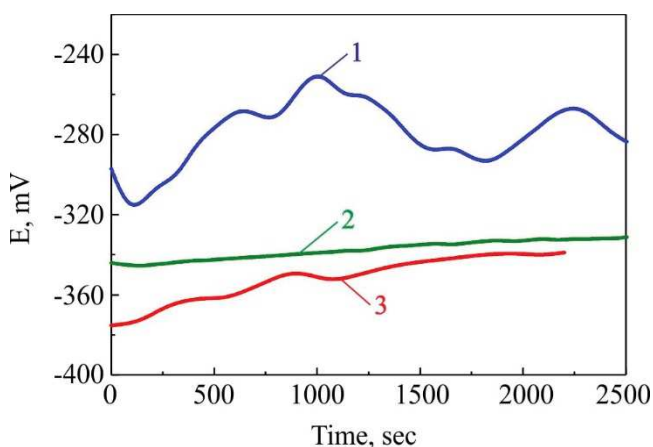

Fig. 5. Time dependence of the corrosion potential of alloys V-8Ti (curve 1), V-15Cr (2), and V-35Cr (3) in 3% NaCl aqueous solution

The corrosion behaviour of the alloys correlates with well-known results on a higher affinity of titanium to oxygen compared with chromium. Titanium is capable of forming dense, uniform and highly adhesive oxide films. While chromium oxides are usually of loose spinel type. Therefore, with almost the same oxygen content, the protective properties of titanium oxides should be better.

Another method used to evaluate the corrosion properties of alloys is the method for obtaining potentiodynamical polarization dependences. This method allows to quantify the corrosion rate and determine the value of the current of the self-dissolution. It allows assessing whether inhibitor acts according to the anode, cathode, or mixed mechanism.

During the study, the potentiodynamic polarization technique for constructing the polarization curves was used. The experiment was conducted at a potential scan rate of 2 mV/s. A silver chloride saturated electrode was used as the reference electrode, and a platinum electrode was used as the auxiliary electrode. The samples of alloys were used as working electrodes. The area of each sample has been determined and isolated by an epoxy polymer.

Using this method, the sections of the passivity plateau, the pitting potentials, the anode and cathode currents were determined. For each alloy, a passivity plateau is observed (Fig. 6), but for the V-8Ti sample, it is accompanied by a large decrease in the anode current density. The pitting potential values for all three alloys are similar and is within the range of -300 to -400 mV. We determined the magnitudes of the corrosion current density of the investigated alloys by the method of extrapolation of rectilinear Tafelian sections of polarization dependences (Fig. 6). As a result, the lowest corrosion current density (0.003 mA/cm^2), which indicates the highest corrosion resistance of this material, was found for the V-8Ti alloy, in contrast to two other alloys (0.006 mA/cm^2 and 0.009 mA/cm^2 for V-15Cr and V-35Cr respectively).
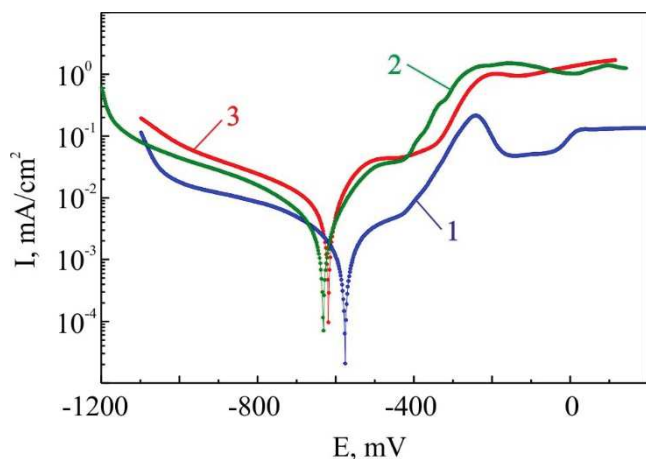

Fig. 6. Polarization dependences for the vanadium alloys V-8Ti (curve 1), V-15Cr (2), and V-35Cr (3) in 3% NaCl aqueous solution

The method of electrochemical impedance spectroscopy (EIS) allows to estimate protective properties of oxide films without destructive influence on samples. It allows to determine the charge transfer resistance (identical to the polarization resistance) and to compare the protective properties of various coatings.

The EIS also allows you to take into account the effect of the electrical resistance on the integral indicator of the impedance system. The frequency dependences of the impedance modulus (Fig. 7a) and the phase angle (Fig. 7b) for vanadium alloys samples in 3% NaCl aqueous solution were obtained.

The values of the modulus Z and the angle θ were recorded in the frequency range of 0.01 Hz to 10,000 Hz. The amplitude of the applied signal was ±10 mV. By using the EIS method (Fig. 7a), it was revealed that the impedance

modulus most depends on the frequency of alternating current in samples of the V-8Ti alloy. The frequency dependences of the impedance modulus of the V-15Cr and V-35Cr alloys are placed somewhat lower. This fact indicates a higher corrosion resistance of the vanadium-titanium alloy in a chloride-containing solution.
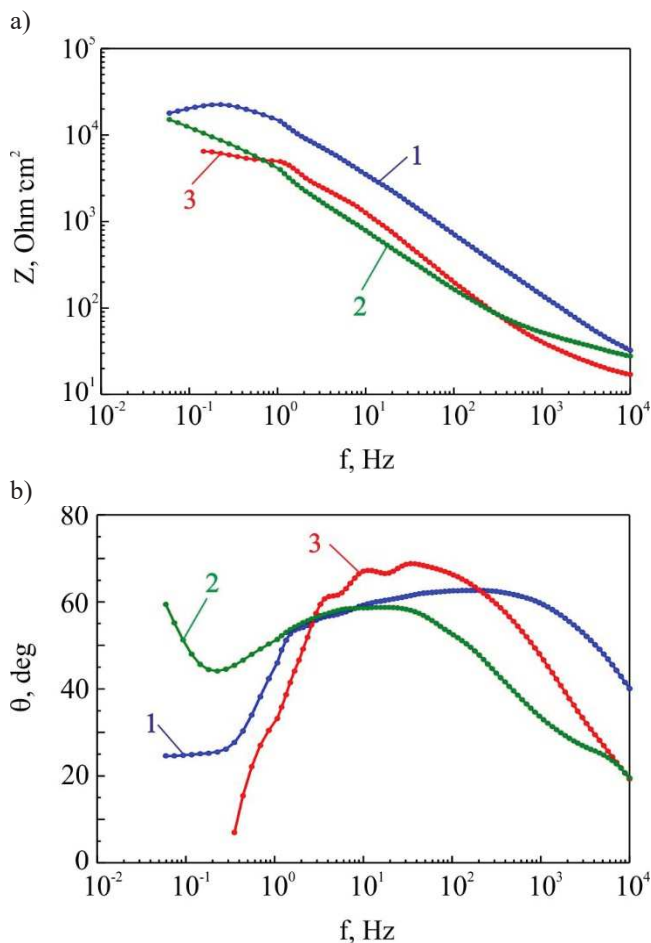

Fig. 7. Frequency dependences of the impedance modulus (a) and of the phase angle (b) for the vanadium alloys V-8Ti (curve 1), V-15Cr (2), and V-35Cr (3) in 3% NaCl aqueous solution

Besides, using the computer software EIS Spectrum Analyzer, the charge transfer resistance of samples of the investigated alloys in the chloride-containing corrosive environment was calculated. It was found that the charge transfer resistances of the vanadium-titanium alloy and alloys V-15Cr and V-35Cr are 20,000 Ohm·cm^2, 16,000 Ohm·cm^2, and 6,500 Ohm·cm^2, respectively. Based on the frequency dependences of the phase angle for the vanadium alloys in 3% NaCl aqueous solution (Fig. 7b), it can be

concluded that the V-8Ti alloy has a denser and defect-free passive oxide film on the surface. In contrast to this, such an oxide film on the surface of the V-15Cr alloy is relatively defective and has low protective properties, possibly due to the presence of oxygen as an impurity in this alloy.

Thus, the impedance spectroscopy data show the highest corrosion resistance of the vanadium-titanium alloy in a highly mineralized chloride-containing solution as compared to the other two vanadium alloys.

4. Conclusions

1. It was found that on the surface of the investigated alloys of V-Ti and V-Cr systems there are periodically dark areas as a result of uneven energy distribution of hydrodynamic impact of nitrogen plasma. In these areas, dendritic crystallites of various sizes were detected for vanadium alloys of composition V-15Cr and V-35Cr, whereas in the V-8Ti alloy, these crystallites have a pronounced cubic shape. Given the chemical composition of the surface layers of these alloys after irradiation with nitrogen plasma, it can be assumed that these inclusions belong to the nitride or oxynitride phases.
2. After irradiation with low-temperature nitrogen plasma, the surface microhardness increased for all investigated vanadium alloys. This can be the result of surface plastic deformation after hydrodynamic impact of nitrogen plasma and due to the formation of secondary phases.
3. The impedance spectroscopy results indicate an increased corrosion resistance of the V-8Ti alloy in a highly mineralized chloride-containing solution as compared to the other two vanadium alloys. This is due to passivation of the surface of this alloy.

Acknowledgements

References

[1] Z.A. Duriagina, T.L. Tepla, Modification of surfaces of special alloys by nitrogen for power engineering, Ukrainian Journal of Mechanical Engineering and Materials Science 1/1 (2015) 99-104.

[2] Z.A. Duryagina, S.A. Bespalov, V.Ya. Pidkova, D.Yu. Polockyj, Examination of the dielectric layers on the structural materials formed by hybrid ion-plasma discharge system, Metallofizika i Noveishie Tekhnologii 33/Spec. iss. (2011) 393-400.

[3] M.I. Pashechko, V.V. Shyrokov, Z.A. Duryahina, Kh.B. Vasyliv, Structure and corrosion-mechanical properties of the surface layers of steels after laser alloying, Materials Science 39/1 (2003) 108-117, DOI: https://doi.org/10.1023/A:1026134714719

[4] Z.A. Duryagina, E.R. Bondar', V.I. Zyryanov, Protection of chromium steel from corrosive effect of $Li_{17}Pb_{83}$ eutectic by diffusion coating, Fizika i Khimiya Obrabotki Materialov 4 (1991) 107-110.

[5] T. Muroga, J.M. Chen, V.M. Chernov, R.J. Kurtz, M.Le Flem, Present status of vanadium alloys for fusion applications, Journal of Nuclear Materials 455/1-3 (2014) 263-268, DOI: https://doi.org/10.1016/j.jnucmat.2014.06.025.

[6] H. Serizawa, H. Ogura, Y. Morisada, H. Fujii, H. Mori, T. Nagasaka, Influence of friction stir welding conditions on joinability of V-alloy/SUS316L dissimilar joint, Nuclear Materials and Energy 15 (2018) 43-47, DOI: https://doi.org/10.1016/j.nme.2018.05.020

[7] R. Li, P. Zhang, X. Li, C. Zhang, J. Zhao, First-principles study of the behavior of O, N and C impurities in vanadium solids, Journal of Nuclear Materials 435/1-3 (2013) 71-76, DOI: https://doi.org/10.1016/j.jnucmat.2012.12.022

[8] P. Zhang, J. Zhao, B. Wen, Vacancy trapping mechanism for multiple hydrogen and helium in beryllium: a first-principles study, Journal of Physics: Condensed Matter 24/9 (2012) 095004, DOI: https://doi.org/10.1088/0953-8984/24/9/095004

[9] X. Wu, X.-S. Kong, Y.-W. You, W. Liu, C.S. Liu, J.-L. Chen, G.-N. Luo, Effect of transition metal impurities on the strength of grain boundaries in vanadium, Journal of Applied Physics 120 (2016) 095901, DOI: https://doi.org/10.1063/1.4961867

[10] P.L. Fauchais, J.V.R. Heberlein, M.I. Boulos, Thermal Spray Fundamentals, Springer, New York, 2014, DOI: https://doi.org/10.1007/978-0-387-68991-3

[11] M. Roy, V.K. Balla, A. Bandyopadhyay, S. Bose, Compositionally graded hydroxyapatite/tricalcium phosphate coating on Ti by laser and induction plasma, Acta Biomaterialia 7/2 (2011) 866-873, DOI: https://doi.org/10.1016/j.actbio.2010.09.016

[12] Z. Xu, X. Liu, P. Zhang, Y. Zhang, G. Zhang, Z. He, Double glow plasma surface alloying and plasma nitriding, Surface and Coatings Technology 201/9-11

(2007) 4822-4825, DOI: https://doi.org/10.1016/j.surfcoat.2006.07.187

[13] H. Kawasumi, Metal surface hardening CO_2 laser, in: E.A. Metzbower (Ed.), Source Book on Applications of the Laser in Metalworking, ASM, Metals Park, Ohio, 1981, 185-195.

[14] M. Popović, M. Novaković, A. Traverse, K. Zhang, N. Bibić, H. Hofsäss, K.P. Lieb, Modifications of reactively sputtered titanium nitride films by argon and vanadium ion implantation: Microstructural and opto-electric properties, Thin Solid Films 531/15 (2013) 189-196, DOI: https://doi.org/10.1016/j.tsf.2013.01.045

[15] J.L. Murray, The Ti-V (Titanium-Vanadium) system, Bulletin of Alloy Phase Diagrams 2 (1981) 48-55, DOI: https://doi.org/10.1007/BF02873703

[16] VEGA 3 SEM Instruction for use, Brno, TESCAN, 2013.

[17] O. Kanoun, Lecture Notes on Impedance Spectroscopy: Measurement, Modeling and Applications, Taylor & Francis Group, London, 2018.